Plant-derived coumarins shape the composition of an *Arabidopsis* synthetic root microbiome

Mathias J. E. E. E. Voges[a,b], Yang Bai[c,1,2,3], Paul Schulze-Lefert[c,d], and Elizabeth S. Sattely[a,e,4]

[a]Department of Chemical Engineering, Stanford University, Stanford, CA 94305; [b]Department of Bioengineering, Stanford University, Stanford, CA 94305; [c]Department of Plant Microbe Interactions, Max Planck Institute for Plant Breeding Research, 50829 Cologne, Germany; [d]Cluster of Excellence on Plant Sciences, Max Planck Institute for Plant Breeding Research, 50829 Cologne, Germany; and [e]Howard Hughes Medical Institute, Stanford University, Stanford, CA 94305

Edited by Jeffery L. Dangl, University of North Carolina, Chapel Hill, NC, and approved May 7, 2019 (received for review December 4, 2018)

The factors that contribute to the composition of the root microbiome and, in turn, affect plant fitness are not well understood. Recent work has highlighted a major contribution of the soil inoculum in determining the composition of the root microbiome. However, plants are known to conditionally exude a diverse array of unique secondary metabolites, that vary among species and environmental conditions and can interact with the surrounding biota. Here, we explore the role of specialized metabolites in dictating which bacteria reside in the rhizosphere. We employed a reduced synthetic community (SynCom) of *Arabidopsis thaliana* root-isolated bacteria to detect community shifts that occur in the absence of the secreted small-molecule phytoalexins, flavonoids, and coumarins. We find that lack of coumarin biosynthesis in *f6′h1* mutant plant lines causes a shift in the root microbial community specifically under iron deficiency. We demonstrate a potential role for iron-mobilizing coumarins in sculpting the *A. thaliana* root bacterial community by inhibiting the proliferation of a relatively abundant *Pseudomonas* species via a redox-mediated mechanism. This work establishes a systematic approach enabling elucidation of specific mechanisms by which plant-derived molecules mediate microbial community composition. Our findings expand on the function of conditionally exuded specialized metabolites and suggest avenues to effectively engineer the rhizosphere with the aim of improving crop growth in iron-limited alkaline soils, which make up a third of the world's arable soils.

plant microbiome | coumarins | synthetic communities | plant specialized metabolism

Up to 25% of photosynthetically fixed carbon is deposited by plant roots into the surrounding soil as diverse C-containing compounds, such as sugars, amino acids, organic acids, and larger rhizodeposits (1–3). These root exudates are thought to provide key nutrients and reducing equivalents for the sustenance and proliferation of soil microbes that are able to utilize them, possibly resulting in the enrichment of specific bacterial taxa at the plant root compared with the soil biome (4). This "rhizosphere effect" has been observed in numerous plant and crop species, most notably in *Avena barbata* (oat) (5), *Zea mays* (maize) (6), *Medicago sativa* (7), and the model plant *Arabidopsis thaliana* (8). For example, studies in oat have revealed a positive correlation between the capacity of a microbe to utilize compounds exuded by the oat root and the microbe's relative abundance at this underground tissue (5). Root microbial assemblages, in turn, affect the fitness of the plant host in varied ways, including by facilitating access to key nutrients (9) and biocontrol activity (10).

Besides excretion of primary metabolites and carbon-rich sugars, we and others have observed that plants conditionally exude a diverse range of unique secondary metabolites (11–13). A number of these molecules have established roles in plant nutrient acquisition and abiotic stress tolerance. For example, in iron-limiting stress conditions, many plants exude small redox-active molecules involved in mobilizing iron via chelation and subsequent reduction, such as the iron-mobilizing coumarins esculetin, fraxetin, and sideretin in *A. thaliana* (12, 14). Less is understood about how secreted plant molecules might mediate cross-kingdom interactions. However, lead examples demonstrate the potential for secreted plant metabolites to modulate the abundance and even the function of specific soil microbiota that, in turn, disadvantage or benefit growth and development of the host plant (15, 16). For example, certain flavonoids exuded by *Glycine max* and *M. sativa* initiate a cascade of molecular events in nitrogen-fixing rhizobia that result in the development of root nodules for bacterial accommodation that ultimately benefit both the plant and microbe (17, 18). In the well-studied Brassicaceae plant family, sulfur-containing phytoalexins limit the growth of pathogenic fungi and conditionally beneficial fungal endophytes, resulting in enhanced plant survival and fitness (13, 19). Despite the important contribution of secondary metabolites to host fitness in ecological and environmental extremes, such as fending off pathogens or nutrient acquisition,

Significance

The root microbiome composition is largely determined by the soil inoculum, with a distinct contribution from the host. The molecular mechanisms with which the host influences its rhizobiome are only beginning to be discovered. Using a hydroponics-based synthetic community approach, we probe how root-exuded specialized metabolites sculpt the root microbiome. We uncover a role for coumarins in structuring the rhizobiome, particularly by limiting the growth of a *Pseudomonas* strain, for which we propose a mechanism of action involving reactive oxygen species. Our findings support the possibility that root-exuded coumarins form a part of the plant's adaptive response to iron deficiency that goes beyond iron mobilization to modulate the rhizobiome, and highlight avenues toward engineering the rhizosphere for plant health.

Author contributions: M.J.E.E.E.V., Y.B., P.S.-L., and E.S.S. designed research; M.J.E.E.E.V. performed research; Y.B. and P.S.-L. contributed new reagents/analytic tools; M.J.E.E.E.V., Y.B., P.S.-L., and E.S.S. analyzed data; and M.J.E.E.E.V. wrote the paper with assistance from P.S.-L. and E.S.S.

The authors declare no conflict of interest.

This article is a PNAS Direct Submission.

[1]Present address: State Key Laboratory of Plant Genomics, Institute of Genetics and Developmental Biology, Innovative Academy of Seed Design, Chinese Academy of Sciences, 100101 Beijing, China.

[2]Present address: CAS-JIC Centre of Excellence for Plant and Microbial Sciences, Institute of Genetics and Developmental Biology, Chinese Academy of Sciences, 100101 Beijing, China.

[3]Present address: College of Advanced Agricultural Sciences, University of Chinese Academy of Sciences, 100039 Beijing, China.

[4]To whom correspondence may be addressed. Email: sattely@stanford.edu.

This article contains supporting information online at www.pnas.org/lookup/suppl/doi:10.1073/pnas.1820691116/-/DCSupplemental.

Published online May 31, 2019.

their impact on the structure of the commensal bacterial assemblage associated with plant roots remains poorly understood.

Establishing causal links between plant metabolites and microbial community composition remains challenging. One technical issue experimentalists face is the difficulty in tracking bacterial strains by 16S rRNA gene surveys in diverse environments, such as soils. In addition, using genetic disruption in the plant host can have pleiotropic effects on plant metabolism, and thus microbial community composition. For example, in a seminal study employing *A. thaliana*, the hormone salicylic acid (SA) was shown to affect the root microbiome profile of plants grown in soils or a gnotobiotic system by employing defense phytohormone mutant lines (20). However, the use of phytohormone mutant lines could have indirect effects on the plant's metabolism, resulting in root microbiome shifts with unexplained causes. Similarly, a recent study presented a possible role for scopoletin in root microbiome assembly (11). This study was limited to describing differential abundances at the operational taxonomic unit (OTU) level (>97% similarity of 16S rRNA), and was thus unable to draw a mechanistic link between exudation of the metabolite of interest and a known root-colonizing bacterial isolate.

Here, we use a synthetic community (SynCom) composed of *A. thaliana* root-derived bacterial commensals to analyze whether *A. thaliana* root-secreted specialized metabolites modulate community composition. The SynCom was designed using strains that (*i*) span the range of taxonomic diversity found at the *A. thaliana* root, (*ii*) can be individually tracked by 16S rRNA gene amplicon analysis, and (*iii*) proliferate in nutrient-rich media (21). This SynCom was used to colonize the roots of both wild-type and biosynthetic mutant plants with genetic disruptions in several major branches of specialized metabolism that result in metabolites that are conditionally secreted from roots and known to contribute to plant fitness under various conditions (22). Specifically, we tested mutant plants deficient in flavonoids (*tt5*) (23), tryptophan-derived defense metabolites (*cyp79Bb2/b3*) (24), methionine-derived defense metabolites (*myb28*) (25), and coumarins (*f6′h1*) (12). To overcome issues arising from the heterogeneity of soils and soil substitutes, a hydroponic growth setup was employed. Among several changes in the abundance of specific community members, we find that a *Pseudomonas* sp. isolate is consistently affected by catecholic coumarins and propose a molecular mechanism of action involving reactive oxygen species (ROS). Taken together, these data showcase a systematic approach to investigate the effect of root-exuded specialized metabolites on the rhizobiome, and reveal a role for conditionally exuded coumarins in sculpting a SynCom at the *A. thaliana* root.

Results

A Distinct Root Microbiome Profile Is Observed for *A. thaliana* Using a Hydroponics-Based Gnotobiotic Setup. A hydroponics-based method developed previously (12) to characterize *A. thaliana* root exudates was used to probe the effects of root-specialized metabolites on microbial communities (Fig. 1*A*). We designed a 22-member SynCom from *A. thaliana* root endophyte isolates collected from loamy soil in Cologne (21) (*SI Appendix*, Table S1). Members of our SynCom span a wide range of the diversity found in the *A. thaliana* root microbiota in terms of family-level taxonomy (26, 27) and were selected such that each can be uniquely identified by 16S rRNA gene amplicon sequencing (*Materials and Methods* and *SI Appendix*, Fig. S1).

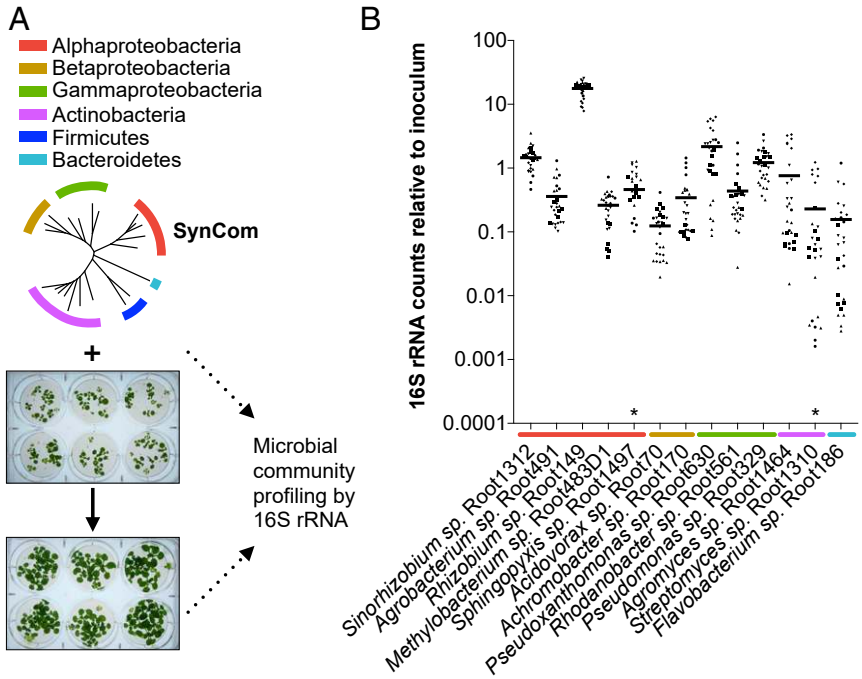

Fig. 1. The gnotobiotic platform used to investigate the effect of plant specialized metabolism on root microbiome composition. (*A*) The media surrounding hydroponically grown 13-d-old *A. thaliana* seedlings was inoculated with a 22-member SynCom (the composition and properties of the SynCom are shown in *SI Appendix*, Fig. S1 and Table S1). The microbial community profile at the 20-d-old root was assessed by 16S rRNA along with the starting inoculum. (*B*) Scatter plot with averages of prominent SynCom members' abundance at the root relative to the starting inoculum as determined by 16S rRNA amplicon count profiling (for strains with reads consistently above two counts after rarefaction as in *SI Appendix*, Fig. S2). Isolates are phylogenetically sorted. Abundances were calculated from 16S rRNA read counts (rarefied to 30,000 reads) of five independent experiments (indicated by the symbol shape). Each data point represents pooled root tissue harvested from two sample wells, each with 16 seeds planted. Values >0.1 suggest an enrichment of that isolate at the root, as a >10-fold increase in colony-forming units is observed in planted media at the time of harvest (*SI Appendix*, Fig. S2*A*). Only SynCom members for which 16S rRNA reads were consistently retrieved from the inoculum and root are shown (*SI Appendix*, Fig. S2*B*). In one experiment, *Sphingopyxis* sp. Root1497 did not colonize the root, while *Streptomyces* sp. Root1310 did (indicated with asterisks). Bacterial phyla are indicated in accordance with the legend in *A*.

A root-mediated shift in community composition (in comparison to the inoculum composition) could be detected in the hydroponics setup using the SynCom (Fig. 1*B*). The growth media surrounding 13-d-old axenically grown seedlings were inoculated to a final composite OD_{600} of 0.005–0.01. After a further 7–8 d of growth, a 10^1- to 10^2-fold increase in total microbial abundance in the hydroponic media was observed, as determined by colony-forming units compared with the starting inoculum and unplanted controls (*SI Appendix*, Fig. S2). The 16S rRNA gene profiling revealed differential relative abundances between SynCom members in the root compared with the starting inoculum. Furthermore, strains that poorly colonized the *A. thaliana* root in monoassociation studies were similarly present at low relative abundances following analysis of 16S rRNA amplicon sequences (*SI Appendix*, Fig. S3). We observed variability in root colonization by some members between experimental batches with independently cultured and assembled SynComs. This was particularly the case for the strains *Sphingopyxis* sp. Root1497, *Microbacterium* sp. Root166, and *Streptomyces* sp. Root1310. Notably, the Proteobacteria, such as *Rhizobium* sp. Root149, *Pseudomonas* sp. Root329, and *Sinorhizobium* sp. Root1312, were consistently enriched at the root, while many Actinobacteria and Firmicutes isolates were not (Fig. 1*B* and *SI Appendix*, Fig. S2). That Proteobacteria are among the strains most abundant at the *Arabidopsis* root is consistent with community composition analyses of plants grown in natural soils and artificial soil substrates (21, 26, 27). However, we cannot exclude the possibility that Firmicutes and some Actinobacteria grow poorly in the plant growth media used (*SI Appendix*, Fig. S3).

Strain Abundances at the Roots of *Arabidopsis* Mutants Deficient in Specialized Metabolite Biosynthesis. Indole- and methionine-derived defense metabolites, flavonoids, and coumarins (Fig. 2*A*) have previously been identified in *A. thaliana* root exudates and found to vary across ecotypes and species (12, 16). These studies suggest that molecules derived from these branches of

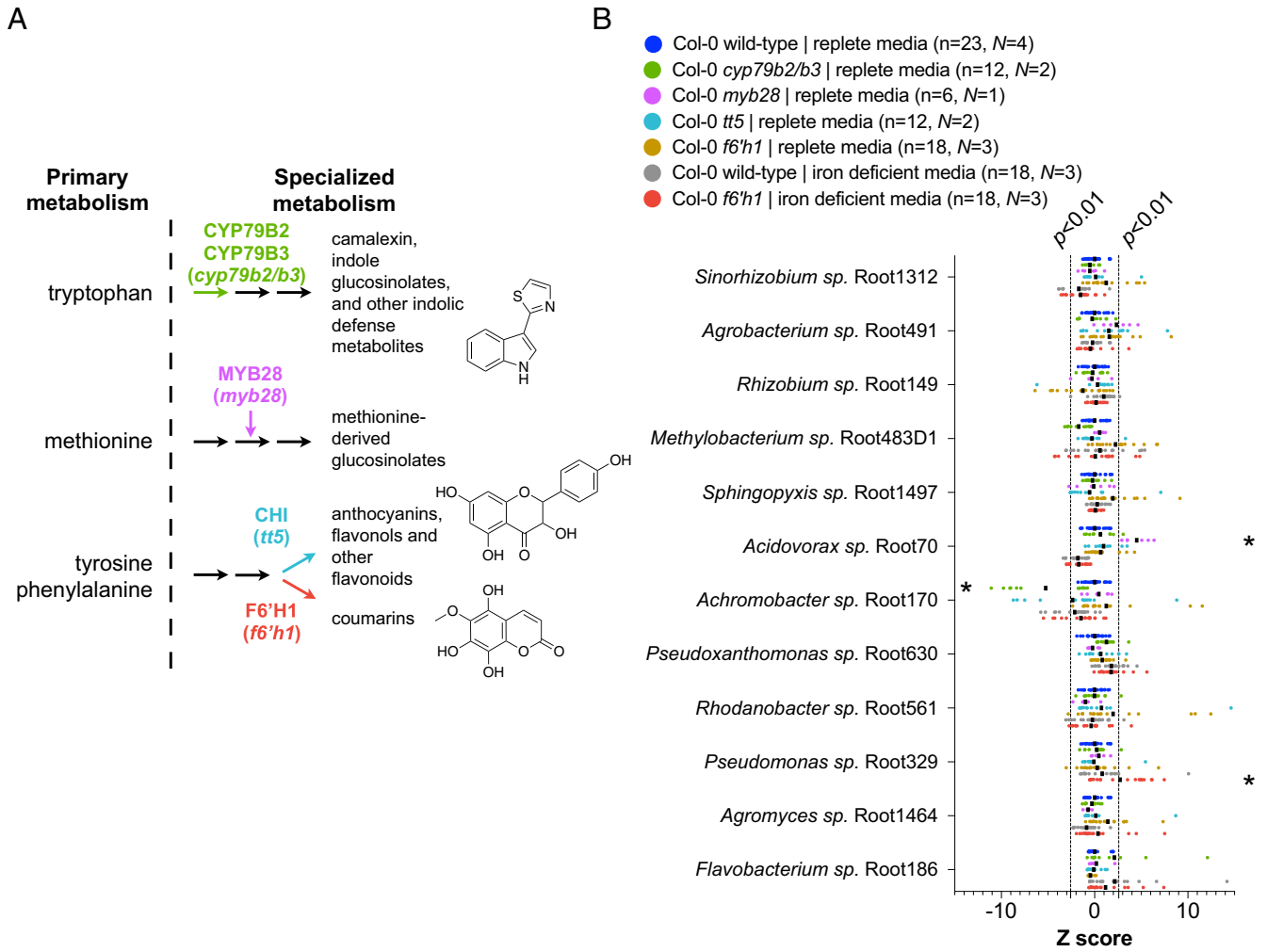

Fig. 2. Root microbial community composition across *A. thaliana* gene disruption lines deficient in major specialized metabolites. (*A*) Schematic of *A. thaliana* metabolism highlighting major pathways toward root-exuded specialized metabolites. Molecular structures representative of specialized metabolism are shown; these are camalexin (*Top*), kaempferol (*Middle*), and sideretin (*Bottom*). The genes investigated are indicated by different colors, with the designation used for corresponding gene disruption lines given in parentheses (the plant lines used are shown in *SI Appendix*, Table S2). (*B*) Scatter plot of strain Z scores comparing each plant genotype with wild type in replete conditions. Here, the strain Z score was defined as the difference between read counts for strains from the roots of mutant lines in each sample (x_{i_mutant}) and corresponding mean of strains from synchronously grown wild-type roots (μ_{i_WT}) in replete media, normalized to the SD of read counts for the strain (σ_{i_WT}) at the wild-type root ($Z = (x_{i\_mutant} - \mu_{i\_WT})/\sigma_{i\_WT}$). Asterisks indicate strains that significantly differ for that genotype. Strains are sorted based on phylogeny. Black dashed lines convey Z scores corresponding to $P = 0.01$ and the mean is given by black bars. Z scores were calculated from 16S rRNA counts (rarefied to 30,000 reads) of *N* independent experiments. Each data point (n) represents pooled root tissue harvested from two sample wells, each with 16 seeds planted.

specialized metabolism may play a role in the local adaptation of the plant to the soil environment and microbial ecology. Furthermore, transcriptomics of the *A. thaliana* root colonized by commensal bacteria revealed up-regulation of genes involved in the biosynthesis of these four branches of specialized metabolism (28). To investigate these specialized metabolites' role in shaping the root microbiome, the SynCom composition across *A. thaliana* lines with mutations in pathway genes required for metabolite biosynthesis was determined. We tested plant lines disrupted for cytochrome P450 79B2 (CYP79B2) and cytochrome P450 79B3 (CYP79B3), known to initiate the indole glucosinolate and camalexin biosynthetic pathways (24); MYB28, the positive transcriptional regulator of aliphatic glucosinolates (25); chalcone isomerase (*tt5*), the committed step toward flavonoid biosynthesis (23); and feruloyl-coenzyme A ortho-hydroxylase 1 (F6′H1), the committed step toward oxidized coumarin biosynthesis (14) (Fig. 2*A*). We employed analysis of similarity (ANOSIM) on Bray–Curtis dissimilarity matrices to assess significance of community composition shifts across mutant genotypes. Overall, no significant changes in the microbial composition of *cyp79b2/b3*, *tt5*, *myb28*, or *f6′h1* compared with wild type in replete conditions were observed (here defined as $P < 0.01$ in ANOSIM). This finding is visually depicted in the degree of sample overlap in nonmetric multidimensional scaling (NMDS) ordination plots (*SI Appendix*, Figs. S4 and S5). To determine strain-level variation, we examined the abundance of individual isolates using Z scores. Here, the Z score was defined as the difference between 16S rRNA amplicon read counts for strains from the roots of mutant lines in each sample and the mean of corresponding strains from synchronously grown wild-type roots, normalized to the SD of read counts from wild-type root isolates ($Z = (x_{i\_mutant} - \mu_{i\_WT})/\sigma_{i\_WT}$). This analysis revealed a significant decrease in the relative abundance of *Achromobacter* sp. Root170 in *cyp79b2/b3* and an increase of *Acidovorax* sp. Root70 in *myb28* in replete growth conditions (Fig. 2*B*; more details on Z-score calculations are provided in *SI Appendix, Materials and Methods*).

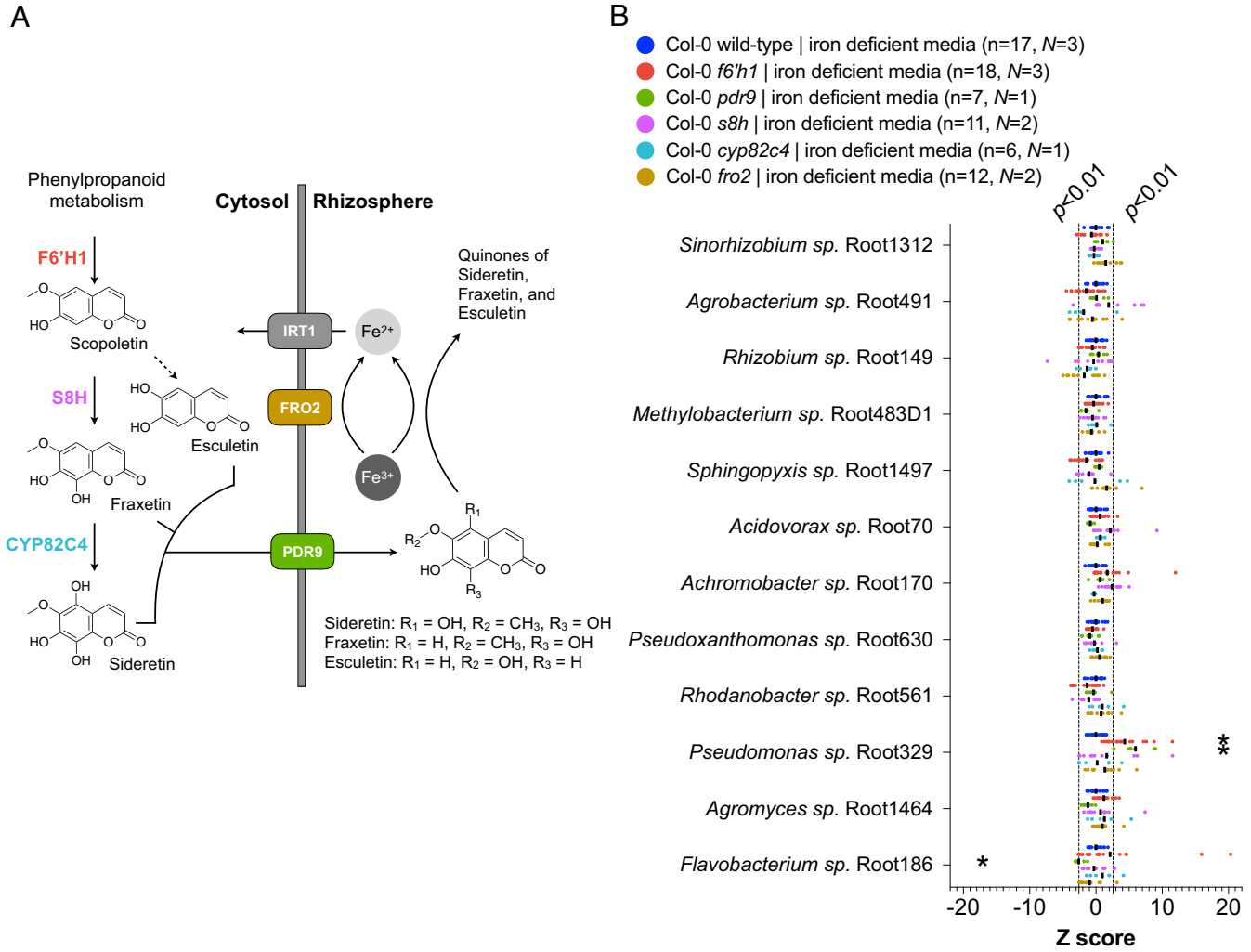

Fig. 3. Root-exuded coumarins shift the microbial community profile at the root. (*A*) Schematic of the *A. thaliana* iron homeostasis genetic repertoire, including genes involved in oxidized coumarin biosynthesis and release. Sideretin, fraxetin, and esculetin are confirmed major coumarins exuded by wild-type roots under iron deficiency at circumneutral pH. (*B*) Scatter plot of strain Z scores comparing each plant genotype with wild type in iron-deficient conditions. Here, the strain Z score was defined as the difference between read counts for strains at the roots of mutant lines and the mean of corresponding strains from synchronously grown wild-type roots in iron-deficient media, normalized to the SD of read counts for the strain at the wild-type root ($Z = (x_{i\_mutant} - \mu_{i\_WT})/\sigma_{i\_WT}$). Strains are sorted based on phylogeny. Black dashed lines convey Z scores corresponding to $P = 0.01$ and the mean is given by black bars. Asterisks indicate strains that significantly differ for that genotype. Z scores were calculated from 16S rRNA counts (rarefied to 30,000 reads) of *N* independent experiments. Each data point (n) represents pooled root tissue harvested from two sample wells, each with 16 seeds planted.

A Shift in Community Composition Is Observed for Plant Lines Lacking Coumarin Biosynthesis When Grown Under Iron Deficiency. Oxidized coumarins downstream of scopoletin, such as esculetin, fraxetin, and sideretin, are typically synthesized and exuded by *A. thaliana* roots under iron deficiency to aid in the mobilization of otherwise biologically inaccessible forms of iron (12) (Fig. 3*A*). F6′H1 represents the dedicated biosynthetic step to coumarin production; mutations in this gene are unable to biosynthesize the coumarins shown in Fig. 3*A* (14). To investigate whether these oxidized coumarins affected the SynCom composition, we compared microbial community profiles of *f6′h1* and wild type in iron-deficient growth conditions (Fig. 2*B*). While there was no significant shift in microbial community profile between wild type and *f6′h1-1* in nutrient-replete conditions, we observed community profiles distinct from wild type in iron-deficient conditions in two of the three experiments (ANOSIM, $P < 0.01$) (*SI Appendix*, Fig. S4). Inspection at the strain level revealed a consistent increase in the relative abundance of *Pseudomonas* sp. Root329 compared with wild type in replete media (Fig. 2*B*) and compared with wild type in iron-deficient media (as determined by Z-score analysis; Fig. 3*B*). In line with the importance of coumarin release in shaping the microbiome composition, we observed community profiles similar to *f6′h1* in *pdr9* (PLEIOTROPIC DRUG RESISTANCE 9) mutants (Fig. 3). The ATP-binding cassette transporter PDR9 is required for the selective exudation of catecholic coumarins (esculetin, fraxetin, and sideretin) under iron deficiency in *Arabidopsis* roots (29).

To confirm that the observed community shift was due to catecholic coumarins, and not to secondary effects brought on by impaired host iron homeostasis in *f6′h1* lines, we included a *fro2* line for root community analysis. Ferric chelate reductase 2 (FRO2) is the principal ferric chelate reductase at the *A. thaliana* root (30) (Fig. 3*A*). The *fro2* line exhibits severe iron deficiency symptoms in alkaline soils with low iron bioavailability. The community profile shifts in *f6′h1-1* lines are significantly dissimilar from wild-type plants, whereas the community profiles of *fro2* lines are not (Fig. 3*B* and *SI Appendix*, Fig. S6), suggesting that the observed community profile shifts are specific to the lack of coumarin biosynthesis in *f6′h1-1*, rather than impaired host iron homeostasis.

Next, root microbial community profiles of insertion mutants in scopoletin-8-hydroxylase (S8H; *s8h*) and in cytochrome P450 82C4 (CYP82C4; *cyp82c4*) were compared with wild type to determine whether any particular coumarin type is exclusively involved in the community shifts observed in *f6′h1* (Fig. 3*A*). The primary coumarin types exuded under iron deficiency differ for each of the mutant lines tested, with wild type exuding primarily sideretin, fraxetin, and esculetin; *cyp82c4* exuding primarily fraxetin and esculetin; and *s8h* exuding mainly esculetin and scopoletin in our hydroponic growth conditions (12) (Fig. 3*A*). Both *s8h* and *cyp82c4* plants assembled a root community profile distinct from *f6′h1-1* or *f6′h1-2*, and more similar to wild type, suggesting that exudation of known *A. thaliana*-biosynthesized catecholic coumarins is sufficient to bring about the community profile observed in wild-type plants (Fig. 3*B* and *SI Appendix*, Fig. S7).

An *f6′h1*-Dependent Increase in Abundance of *Pseudomonas* sp. Root329 Is Consistent and Robust Across Different SynCom Compositions. Upon closer inspection of the relative abundances for individual bacterial strains at the root of wild type and *f6′h1*, *Pseudomonas* sp. Root329 was found to consistently respond positively to lines that lack biosynthesis and release of oxidized coumarins. In contrast, some root-colonizing bacteria tended toward an unchanged or, in some cases, negative response (*Agrobacterium* sp. Root491; Figs. 3*B* and 4*A*). Such compensatory shifts are expected in community profiling by 16S rRNA gene amplicon sequencing, making it a challenge to assess the direction of causality. To address whether *Pseudomonas* sp. Root329 is directly affected by plant-derived coumarins, we (*i*) performed in silico rescaling and NMDS by omitting 16S rRNA gene amplicon reads belonging to *Pseudomonas* sp. Root329 before rarefying and (*ii*) tested whether an increase in *Pseudomonas* sp. Root329 was robust across SynComs of varying size and composition. Removing *Pseudomonas* sp. Root329 by in silico rescaling substantially diminished the community profile shift between wild type and *f6′h1* based on NMDS and ANOSIM (*SI Appendix*, Fig. S8*A*). Next, by either removing the read count-dominant *Rhizobium* sp. Root149 or reducing the size of the SynCom to 14 members, the increase in *Pseudomonas* sp. Root329 persisted (*SI Appendix*, Fig. S8*B*). Furthermore, an increase in *Pseudomonas* sp. Root329 persisted when the community consisted solely of two members. Notably, by reducing the size of the SynCom, a more pronounced increase in abundance for *Acidovorax* sp. Root70 at the *f6′h1* root was observed.

The *f6′h1* Microbial Community Profile is Partially Shifted to that of Wild-Type by Addition of Coumarins. We assessed the microbial community profiles of *f6′h1* lines grown in the presence of scopoletin, fraxetin, or sideretin under iron-deficient conditions (Fig. 4*A* and *SI Appendix*, Fig. S9). *Pseudomonas* sp. Root329 became less abundant at the *f6′h1* root with the addition of either coumarin, while the increase in *Acidovorax* sp. Root70 could be abolished by the addition of fraxetin. Interestingly, increases in the relative abundance of *Agrobacterium* sp. Root491, *Methylobacterium* sp. Root483D1, *Agromyces* sp. Root1464, and *Streptomyces* sp. Root1310 were observed upon addition of either coumarin, possibly due to growth on coumarins, or degradation products, as substrate. Appreciable levels of sideretin were observed in the media of *f6′h1* plants that were chemically complemented with scopoletin, consistent with previous studies (14), suggesting that the community shifts observed may also be caused by biosynthetic conversion of the coumarin types added.

***Pseudomonas* sp. Root329 Growth Is Inhibited by Iron-Mobilizing Coumarins in Vitro.** To determine if F6′H1-dependent coumarins directly impact the growth of bacterial isolates that comprise the SynCom, we analyzed the sensitivity of the major coumarin-responsive root-proliferating SynCom members to chemically-pure samples of scopoletin, fraxetin, and sideretin in vitro. Notably, severe growth inhibition of *Pseudomonas* sp. Root329 by the predominant wild-type coumarin sideretin, and moderate inhibition by fraxetin were observed using a halo inhibition assay (Fig. 4*B*). This phenomenon was not observed for *Pseudomonas simiae* WCS417, a host-beneficial strain similarly within the *Pseudomonas fluorescens* clade. The differentially abundant strains *Rhizobium* sp. Root149 and *Agrobacterium* sp. Root491 ($P < 0.05$) were not comparably affected by either coumarin; however, a faint ring of apparent growth inhibition was observed surrounding fraxetin-infused discs for both.

We hypothesized that some oxidized coumarins' molecular structures, harboring a reduced catechol moiety, allow for the reduction of oxygen to ROS, which are known potent antimicrobials. Hydrogen peroxide was generated by the catecholic coumarins sideretin, fraxetin, and esculetin in iron-deficient Murashige and Skoog media over a 24-h period, but not for scopoletin or isofraxidin, both of which lack redox functionality (*SI Appendix*, Fig. S10). In support of a model for coumarin-mediated antimicrobial activity via hydrogen peroxide, the inhibitory activity of sideretin on *Pseudomonas* sp. Root329 could be abolished with addition of catalase (Fig. 4*C*). Notably, the antimicrobial activity of sideretin could further be reduced by the addition of soluble iron (Fig. 4*C*). These findings suggest that peroxide is generated by catecholic coumarins when iron is scarce, the typical environment in which iron-mobilizing coumarins are biosynthesized and exuded by the *A. thaliana* root. Sideretin was the most potent hydrogen peroxide generator at short time scales (*SI Appendix*, Fig. S10), which may explain its antimicrobial effect on *Pseudomonas* sp. Root329 in the nutrient-agar assay, which was performed over a 24-h timespan. Further in support of an ROS-mediated mechanism of inhibition,

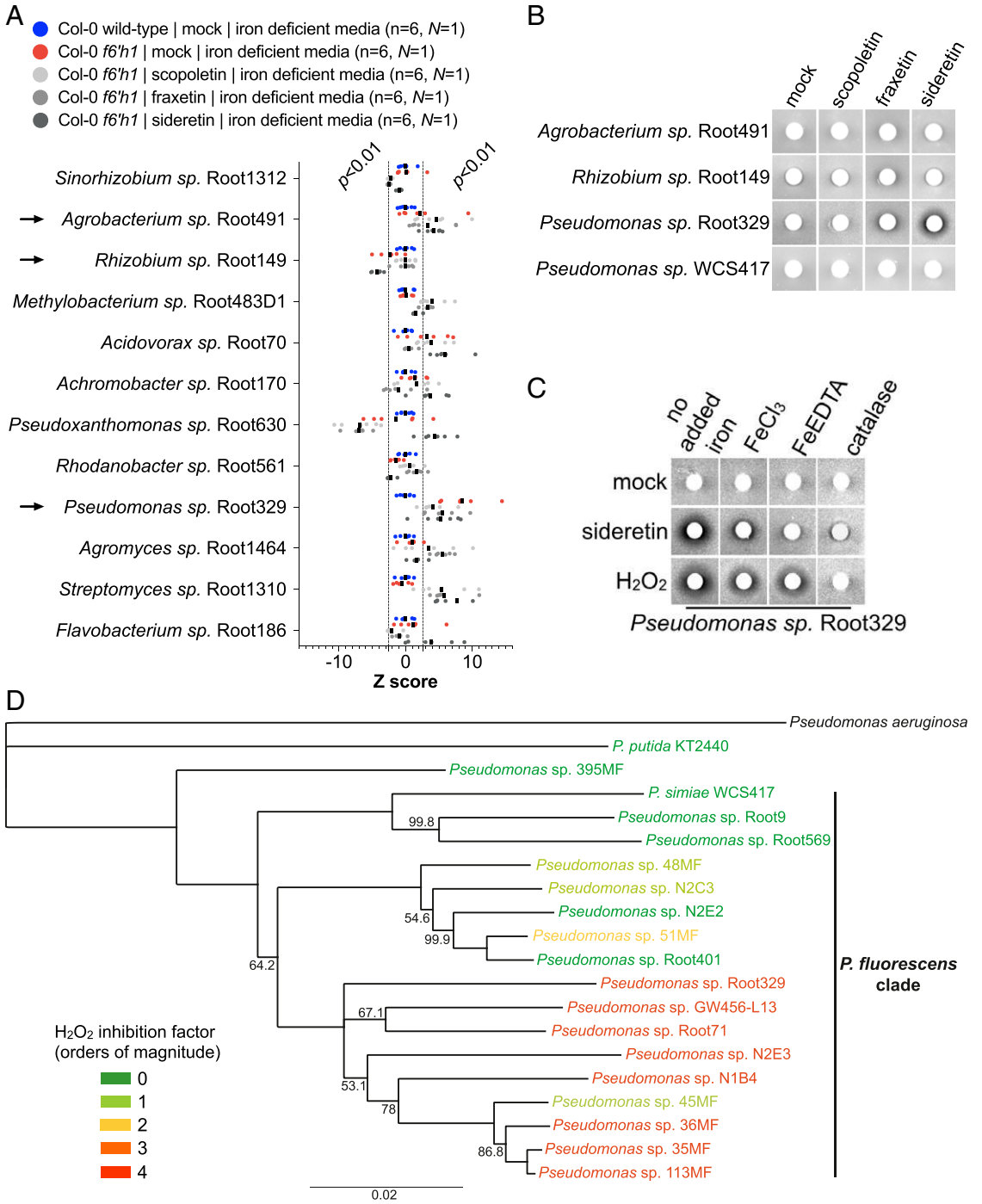

Fig. 4. Purified coumarins partially shift the microbial community to the composition found in wild-type plants, and specifically inhibit the growth of the differentially abundant *Pseudomonas* sp. Root329 isolate via an ROS-mediated mechanism. (*A*) Addition of 100 μM purified oxidized coumarins to the growth media of *f6′h1* lines partially phenocopies wild-type community composition. A scatter plot of Z scores comparing each treatment with wild type in iron-deficient conditions is shown. Z scores are calculated for each strain's abundance at the mutant plant root compared with its abundance at synchronously grown wild-type roots. Black dashed lines convey Z scores corresponding to $P = 0.01$ and the mean is given by black bars. Z scores were calculated from rarefied 16S rRNA counts (30,000 reads per sample). Each data point (n) represents pooled root tissue harvested from two sample wells, each with 16 seeds planted. In comparison to Figs. 2*B* and 3*B*, this analysis did not include *Sphingopyxis* sp. Root1497 (for which reads were consistently below the threshold of three counts) and did include *Streptomyces* sp. Root1310. (*B*) Assays of bacterial growth inhibition surrounding 5-mm filter discs (white circles) infused with dimethyl sulfoxide (DMSO; control) or 10 mM scopoletin, fraxetin, or sideretin (all in 10% DMSO). Bacteria were inoculated into nutrient-agar plates, and filter discs were placed on top of agar. Images were taken after 48 h of growth at 30 °C. The extent of the dark zones surrounding the filter discs represents the degree of bacterial growth inhibition. The experiment was repeated three times with similar results. (*C*) Bacterial growth surrounding filter discs infused with DMSO (control), sideretin, or hydrogen peroxide at 5 mM (all in 10% DMSO). The conditionality of sideretin-mediated growth inhibition was assessed by addition of insoluble iron ($FeCl_3$), soluble iron (Fe-EDTA), or catalase to nutrient-agar plates before inoculation. (*D*) Degree of growth inhibition following H_2O_2 challenge observed for a range of pseudomonads of varied origin. Colors (green to red) represent the magnitude of inhibition observed (*SI Appendix*, Fig. S12). The phylogenetic tree was generated by neighbor joining using the housekeeping genes DNA gyrase (*gyrB*), citrate synthase (*gltA*), and DNA polymerase sigma-70 (*rpoD*). Only consensus support percentages deviating from 100 are shown at the nodes (1,000 tree resamplings in total).

we challenged the most abundant SynCom members at the root with hydrogen peroxide and found that *Pseudomonas* sp. Root329 and *Acidovorax* sp. Root70 were the most affected (based on differential colony-forming unit counts) (*SI Appendix*, Fig. S11). These findings were in line with strains enriched at the *f6′h1* root.

Finally, we investigated the degree to which a range of pseudomonads isolated from the roots of *A. thaliana* grown in Cologne loamy soils, the Mason Farm Preserve in North Carolina, and ground water in Oak Ridge, Tennessee, tolerated H_2O_2 (*SI Appendix*, Table S3 and Fig. S12). Many pseudomonads belonged to the *P. fluorescens* clade and were more than 97% similar at the 16S rRNA locus, so could not be distinguishable at the OTU level. Large differences in the degree of H_2O_2 tolerance were observed for these strains, with a subclade of pseudomonads exhibiting more pronounced sensitivity (Fig. 4*D*).

Discussion

Studies into the host factors that shape the *A. thaliana* rhizosphere community structure have been few, with pioneering work showing that SA is an important player modulating root community composition (20). In contrast to phytohormones, a recent study has correlated microbial growth at the root of oat to the microbe's ability to utilize compounds found to be exuded (5). In general, it was found that utilization of aromatic amino acids is highly correlated with growth at the root. These examples provided impetus for investigating the role of the broader range of diverse metabolites exuded from plant roots on the composition and function of the root microbiome.

By employing a SynCom, the importance of specialized metabolites on microbial community composition could readily be investigated. Of the mutant lines investigated, we find significant changes in relative microbial abundances for coumarin biosynthesis mutants, specifically under iron-limiting conditions. Notably, we find an average 3-fold increased RA of *Pseudomonas* sp. Root329 for plant lines devoid of coumarin biosynthesis or exudation, and provide evidence that this change in relative abundance could be due to this strain's sensitivity to the major catecholic coumarins produced by iron-deficient wild-type plants. As a rough comparison, the changes in relative abundances observed in this study are on par with those observed in previous studies utilizing SynComs. For example, an increase in *Terracoccus* sp. relative abundance (RA) of about 2-fold, and a 3-fold decrease in *Mitsuria* sp. RA upon addition of SA to the roots of *Arabidopsis* have been shown to correspond to these strains' growth response to SA in vitro (20).

Our study provides direct evidence that specialized metabolites can cause reproducible changes in community composition of plant roots. While such interactions are more complex in soil-grown plants, a hydroponic system using a defined bacterial community provides clear evidence that relatively small changes in the secretion of specialized metabolites could impact microbial community structure—evidence that can subsequently be validated in natural soils. For example, in light of our data, one possible explanation for the observed variation of communities in the roots of *f6′h1* plants grown in natural soil (11) compared with those of wild type could be explained by catecholic coumarins produced under iron limitation: esculetin, fraxetin, and sideretin. Interestingly, the *Pseudomonas* genus was not differentially abundant in this study of *f6′h1* plants in natural soils (11). In addition to the unknown effects chemically complex soils may have on coumarin activity, our finding that *Pseudomonas* sp. isolates within the same OTU exhibit varying degrees of sensitivity to fraxetin and sideretin, and to hydrogen peroxide in general, may explain this discrepancy. In our study, the use of a defined SynCom facilitated the discovery of a mechanism of action within the rhizosphere that may have otherwise been overlooked.

We propose that the catechol moiety of iron-mobilizing coumarins facilitates redox reactions that can both mobilize ferric iron and generate ROS, such as hydrogen peroxide, with detrimental effects on microbial proliferation. Similar antimicrobial mechanisms of action have been described for phenazines produced by some pseudomonads: These redox-active small molecules' functionality (either generation of ROS or oxidation by metal ions) is determined by the surrounding iron and oxygen levels (31). ROS have been implicated in the mechanism of action for a number of antimicrobials, suggesting that the mechanisms underlying tolerance to catecholic coumarins may be similar to those of known antimicrobials (32). Furthermore, a number of studies have revealed a link between microbial iron homeostasis and sensitivity to ROS, mainly due to the important role iron plays in bacterial respiration and its involvement in Fenton chemistry within the cell (33).

Bacteria harbor sophisticated mechanisms for iron mobilization and sequestration that, in turn, may have multifaceted effects on host fitness (34, 35). Root bacterial community shifts brought on by iron-mobilizing coumarins could bestow an adaptation to the host plant experiencing iron deficiency, for example, by specifically fending off strong microbial competitors for iron. It has previously been shown that scopoletin could inhibit the growth of fungal pathogens (11). Whether this is also the case for the catecholic coumarins tested here is not yet known. The intriguing possibility exists that plants have specialized to, depending on the neighboring biota, exude intermediates of the same metabolic pathway to modulate the abundances of microbes spanning a large phylogenetic range.

Root-associated bacteria may have evolved mechanisms to sense coumarins that may prove adaptive to the host plant exhibiting iron-deficiency symptoms. We explored this possibility using an agar plate-based assay to assess seedling growth upon inoculation with SynCom members under iron deficiency. While we observed seedling growth promotion upon inoculation of the full SynCom for wild-type plants (*SI Appendix*, Fig. S13), these effects were also conferred by the majority of individual SynCom members in monoassociation experiments (with the exception of the Firmicutes, which proliferate poorly at the root; *SI Appendix*, Fig. S14). Furthermore, we observed no significant difference in growth of wild-type and *f6′h1* seedlings inoculated with *Pseudomonas* sp. Root329, *Rhizobium* sp. Root149 (an isolate that did not display significant RA shifts in *f6′h1*), or plants inoculated with equal densities of both strains (*SI Appendix*, Fig. S15). It remains possible, however, that a plant growth benefit via host-induced community shifts may be observed in more complex microcosms or soils. Future work should investigate the transcriptional response of microbial isolates to coumarins to identify responsive genes, which may offer insights into the molecular mechanisms underpinning seedling growth promotion.

We demonstrate here the promise of employing genetic disruption mutants and SynComs to identify the specific molecular players that sculpt the rhizosphere microbiome. In particular, the ability to track individual members of SynComs facilitates subsequent investigations of the underlying molecular mechanism in vitro (36). A better understanding of the molecular mechanisms required for bacterial colonization of the root and rhizosphere will facilitate efforts toward engineering host-beneficial microbial consortia. Our finding that proliferation of specific microbial strains is affected by iron-mobilizing coumarins can be used to effectively engineer the rhizosphere to improve crop growth in alkaline soils, which make up a third of the world's arable soils (37).

Materials and Methods

A. thaliana seeds were surface-sterilized with 70% ethanol and 50% bleach prior to germination in the hydroponics platform. All SynCom strains were grown to saturation in quarter-strength tryptic soy broth and washed with

phosphate-buffered saline before root inoculation. Full details of materials and methods are provided in *SI Appendix*.

ACKNOWLEDGMENTS. We thank K. Huang, J. Rajniak, R. Garrido-Oter, M. Hashimoto, and H. Inoue for valuable discussions, and S. Long, S. Sirk, A. Denisin, A. Klein, C. Liou, R. Nett, and F. Hol for valuable feedback on the manuscript. We thank X. Ji for technical assistance with Illumina sequencing at the Stanford Functional Genomics Facility and H. Inoue for help in developing seedling growth promotion assays. M.J.E.E.E.V. acknowledges support from the Stanford Bio-X Graduate Fellowship. This work was supported by HHMI and Simons Foundation Grant 55108565 and by NIH DP2 Grant AT008321 (to E.S.S.).

1. N. M. van Dam, H. J. Bouwmeester, Metabolomics in the rhizosphere: Tapping into belowground chemical communication. *Trends Plant Sci.* **21**, 256–265 (2016).
2. H. Massalha, E. Korenblum, D. Tholl, A. Aharoni, Small molecules below-ground: The role of specialized metabolites in the rhizosphere. *Plant J.* **90**, 788–807 (2017).
3. C. Nguyen, Rhizodeposition of organic C by plants: Mechanisms and controls. *Agronomie* **23**, 375–396 (2003).
4. A. Gunina, Y. Kuzyakov, Sugars in soil and sweets for microorganisms: Review of origin, content, composition and fate. *Soil Biol. Biochem.* **90**, 87–100 (2015).
5. K. Zhalnina *et al*., Dynamic root exudate chemistry and microbial substrate preferences drive patterns in rhizosphere microbial community assembly. *Nat. Microbiol.* **3**, 470–480 (2018).
6. W. A. Walters *et al*., Large-scale replicated field study of maize rhizosphere identifies heritable microbes. *Proc. Natl. Acad. Sci. U.S.A.* **115**, 7368–7373 (2018).
7. R. L. Berendsen, C. M. J. Pieterse, P. A. H. M. Bakker, The rhizosphere microbiome and plant health. *Trends Plant Sci.* **17**, 478–486 (2012).
8. S. A. Micallef, M. P. Shiaris, A. Colón-Carmona, Influence of Arabidopsis thaliana accessions on rhizobacterial communities and natural variation in root exudates. *J. Exp. Bot.* **60**, 1729–1742 (2009).
9. O. M. Finkel, G. Castrillo, S. Herrera Paredes, I. Salas González, J. L. Dangl, Understanding and exploiting plant beneficial microbes. *Curr. Opin. Plant Biol.* **38**, 155–163 (2017).
10. P. Durán *et al*., Microbial interkingdom interactions in roots promote Arabidopsis survival. *Cell* **175**, 973–983.e14 (2018).
11. I. A. Stringlis *et al*., MYB72-dependent coumarin exudation shapes root microbiome assembly to promote plant health. *Proc. Natl. Acad. Sci. U.S.A.* **115**, E5213–E5222 (2018).
12. J. Rajniak *et al*., Biosynthesis of redox-active metabolites in response to iron deficiency in plants. *Nat. Chem. Biol.* **14**, 442–450 (2018).
13. P. Bednarek *et al*., A glucosinolate metabolism pathway in living plant cells mediates broad-spectrum antifungal defense. *Science* **323**, 101–106 (2009).
14. N. B. Schmid *et al*., Feruloyl-CoA 6′-Hydroxylase1-dependent coumarins mediate iron acquisition from alkaline substrates in Arabidopsis. *Plant Physiol.* **164**, 160–172 (2014).
15. N. Strehmel, C. Böttcher, S. Schmidt, D. Scheel, Profiling of secondary metabolites in root exudates of Arabidopsis thaliana. *Phytochemistry* **108**, 35–46 (2014).
16. S. Mönchgesang *et al*, Natural variation of root exudates in Arabidopsis thaliana-linking metabolomic and genomic data. *Sci. Rep.* **6**, 29033 (2016).
17. N. K. Peters, J. W. Frost, S. R. Long, A plant flavone, luteolin, induces expression of Rhizobium meliloti nodulation genes. *Science* **233**, 977–980 (1986).
18. R. Zgadzaj *et al*., Root nodule symbiosis in Lotus japonicus drives the establishment of distinctive rhizosphere, root, and nodule bacterial communities. *Proc. Natl. Acad. Sci. U.S.A.* **113**, E7996–E8005 (2016).
19. K. Hiruma *et al*., Root endophyte Colletotrichum tofieldiae confers plant fitness benefits that are phosphate status dependent. *Cell* **165**, 464–474 (2016).
20. S. L. Lebeis *et al*., Salicylic acid modulates colonization of the root microbiome by specific bacterial taxa. *Science* **349**, 860–864 (2015).
21. Y. Bai *et al*., Functional overlap of the Arabidopsis leaf and root microbiota. *Nature* **528**, 364–369 (2015).
22. J. C. D'Auria, J. Gershenzon, The secondary metabolism of Arabidopsis thaliana: Growing like a weed. *Curr. Opin. Plant Biol.* **8**, 308–316 (2005).
23. B. W. Shirley *et al*., Analysis of Arabidopsis mutants deficient in flavonoid biosynthesis. *Plant J.* **8**, 659–671 (1995).
24. A. P. Klein, G. Anarat-Cappillino, E. S. Sattely, Minimum set of cytochromes P450 for reconstituting the biosynthesis of camalexin, a major Arabidopsis antibiotic. *Angew. Chem. Int. Ed. Engl.* **52**, 13625–13628 (2013).
25. T. Gigolashvili, R. Yatusevich, B. Berger, C. Müller, U.-I. Flügge, The R2R3-MYB transcription factor HAG1/MYB28 is a regulator of methionine-derived glucosinolate biosynthesis in Arabidopsis thaliana. *Plant J.* **51**, 247–261 (2007).
26. D. S. Lundberg *et al*., Defining the core Arabidopsis thaliana root microbiome. *Nature* **488**, 86–90 (2012).
27. D. Bulgarelli *et al*., Revealing structure and assembly cues for Arabidopsis root-inhabiting bacterial microbiota. *Nature* **488**, 91–95 (2012).
28. C. Zamioudis *et al*., Rhizobacterial volatiles and photosynthesis-related signals coordinate MYB72 expression in Arabidopsis roots during onset of induced systemic resistance and iron-deficiency responses. *Plant J.* **84**, 309–322 (2015).
29. J. Ziegler, S. Schmidt, N. Strehmel, D. Scheel, S. Abel, Arabidopsis transporter ABCG37/PDR9 contributes primarily highly oxygenated coumarins to root exudation. *Sci. Rep.* **7**, 3704 (2017).
30. E. L. Connolly, N. H. Campbell, N. Grotz, C. L. Prichard, M. L. Guerinot, Overexpression of the FRO2 ferric chelate reductase confers tolerance to growth on low iron and uncovers posttranscriptional control. *Plant Physiol.* **133**, 1102–1110 (2003).
31. Y. Wang, D. K. Newman, Redox reactions of phenazine antibiotics with ferric (hydr) oxides and molecular oxygen. *Environ. Sci. Technol.* **42**, 2380–2386 (2008).
32. D. J. Dwyer *et al*., Antibiotics induce redox-related physiological alterations as part of their lethality. *Proc. Natl. Acad. Sci. U.S.A.* **111**, E2100–E2109 (2014).
33. J. Yeom, J. A. Imlay, W. Park, Iron homeostasis affects antibiotic-mediated cell death in Pseudomonas species. *J. Biol. Chem.* **285**, 22689–22695 (2010).
34. G. Vansuyt, A. Robin, J.-F. Briat, C. Curie, P. Lemanceau, Iron acquisition from Fe-pyoverdine by Arabidopsis thaliana. *Mol. Plant Microbe Interact.* **20**, 441–447 (2007).
35. E. H. Verbon *et al*., Iron and immunity. *Annu. Rev. Phytopathol.* **55**, 355–375 (2017).
36. S. Herrera Paredes *et al*., Design of synthetic bacterial communities for predictable plant phenotypes. *PLoS Biol.* **16**, e2003962 (2018).
37. Y. Dessaux, C. Grandclément, D. Faure, Engineering the rhizosphere. *Trends Plant Sci.* **21**, 266–278 (2016).